Histone H3K27me3 Demethylase act as Key Regulator of Stem Cell Markers in Matrix Detached Cancer Cells

Mohammed Razeeth (✉ razeeth.new@gmail.com)

King Abdulaziz University   https://orcid.org/0000-0002-4711-1483

Mazin Zamzami

King Abdulaziz University

Hani Choudhry

King Abdulaziz University

Firoz Ahmed

King Abdulaziz University

Bushra Ateeq

Indian Institute of Technology Kanpur

Mohammad Imran Khan

King Abdulaziz University

Original Article

Abstract

Metastasis of cancer cells requires detachment from matrix (Extra Cellular Matrix) to seed cancer cells in a distant organ. Hypoxia is prevalent in matrix detached cancer cells, are bound for metastasis. Studies have established hypoxia as chromatin modifier, as it transcriptionally controls expression of various histone demethylases (KDMs), therefore we hypothesized that hypoxia can modulate the expression of KDMs in matrix detached cancer cells. Results from our study showed that in hypoxic matrix detached cancer cells of different origins, expression and activity of KDM6B (a H3K27me3 histone demethylase) was consistently increased. Simultaneously, we found increased expression of cancer stem cells (CSCs) markers in hypoxic matrix detached cancer cells. Targeting KDM6B by using a specific inhibitor reduces the expression of CSCs markers namely SOX-2, SOX-9 and CD44 in matrix detached cancer cells. We found that KDM6B occupies the promoter region of both SOX-2 and CD44 and thereby regulate their expression. Surprisingly, we also noticed that in a feedback loop HIF1α was transcriptionally regulated by KDM6B in matrix detached cancer cells. Lastly, we observed a significant positive association between KDM6B and HIF1α in various cancer types. Overall, we found, that matrix detachment induces hypoxia, modulates epigenome to promote KDM6B activity to positively regulate expression of SOX2, CD44 and HIF1α in matrix detached conditions. We believe that KDM6B can be developed as a therapeutic target for elimination of matrix detached cancer cells, bound for metastatic events.

Introduction

Normal epithelial cells that are non-tumorigenic and are anchorage-dependent i.e. they attach well with the matrix for obtaining nutrition and physiological ques. However, tumorigenic epithelial cells require detachment from matrix in order to move to distinct sites of the body for initiation of metastasis [1-3]. Several studies have shown that loss of matrix detachment leads to vast changes at both molecular and cellular levels and these changes are attributed to matrix detached cells to became anoikis resistance[3,4]. Matrix detached cells overcome anoikis condition through several pathways one of them is related to epithelial-mesenchymal transition of ECM detached epithelial cells[5,6].

Matrix detached cancer cells are often supported by hypoxia that facilitates metabolic switch from oxidative phosphorylation to glycolysis, in order to maintain cell proliferation and vitality [7]. In addition to this, the transcriptomic adjustment of the circulating, matrix detached tumorigenic cells are also documented due to diverge epigenetic changes at DNA and histone levels [8-10] .

Hypoxia is a well-recognized modulator of epigenetic landscape. The hypoxic transcription factor HIF-1α alters chromatin in different ways, primarily by regulating the expression level of several JmjC- Jumonji-domain histone demethylases (KDMs) [11-14]. Further, almost all of the Jumonji-type KDMs are members of the 2-oxoglutarate-dependent dioxygenase family (2-OGDO) and therefore are highly dependent on oxygen levels along with "2-oxoglutarate", a Krebs cycle intermediate to catalyze their enzymatic reactions. Most KDM enzymes are structurally similar to the HIF hydroxylase Factor Inhibiting HIF-1 (FIH), suggesting that KDM enzymes may act as molecular oxygen sensors in the cell [15,16]. These findings

suggest that hypoxia can modulate the gene expression by modulating the expression and activity of KDMs. However, it is not yet clear whether hypoxia, is crucial element of matrix detached cancer cells facilitates or directly participates in the epigenetic changes, might occurs in matrix detached cancer cells.

Therefore, in the current study we aimed to explore the impact of matrix detachment on epigenome mainly hypoxia regulated KDM(s) in various cancer types. Also, we aimed to assess the role of identified KDM(s) in maintaining the stemness and survival of matrix detached cancer cells.

Materials And Methods

Cell lines and culture

Various cancer cell lines were maintained in Dulbecco's Modified Eagle's Medium (DMEM) media supplemented with 10 % FBS and 1% penicillin-streptomycin (Invitrogen) at 37°C in 5% CO_2. All the cell lines namely HCT116, HeLa, and 22R1used in the current study were obtained from ATCC (USA). The cells were grown up to 70- 90% confluence and media was changed every two days. The cell lines were routinely checked for any mycoplasma contamination.

Matrix detachment model of stemness

We have followed the well-established method of cell detachment model in our experiments [17,18] Briefly, cells were grown in ultra-low attachment plate obtained from Corning (Sigma) in CO_2 incubator at 37°C. The assessments of matrix detachment were done in cell suspension culture. Cells were dislodged by simple agitation in presence of trypsin, followed with washing with PBS, resuspended at 0.5×10^6 cells/ml in serum-free culture media containing BSA and finally were cultured in ultra-low attachment plate for at 37°C for various time points, which results in formation of spheroids. The spheroids were treated with either vehicle control or with different concentration of GSK J4 (Abcam-144396, Cambridge, MA USA) for 5 days. The images were captured by using Nikon (USA) inverted light microscope. Images were analyzed for size measurement using image J software (https://imagej.net/Invasion_assay).

Real-time qPCR analysis for mRNA expression

Briefly, RNA was extracted from all the cell lines at the end of different experimental conditions by using Rneasy kit (Qiagen), and reverse transcribed with a High capacity cDNA Reverse Transcription kit (applied biosystems). cDNA (1-100ng) was amplified in triplicate using gene specific primers (Table-1). Threshold cycle (C_T) values obtained from the instrument's software were used to calculate the fold change of the respective mRNAs. ΔC_T was calculated by subtracting the C_T value of the housekeeping gene from that of the mRNA of interest. $\Delta\Delta C_T$ for each mRNA was then calculated by subtracting the C_T value of the control from the experimental value. Fold change was calculated by the formula $2^{-\Delta\Delta CT}$.

Protein extraction and western blot analysis

Various cancer cells (HCT116, HeLa, and 22RΩ1) were cultured in T_{75} flask (1×10^6 / flask). After 24 hours cells of cell plating in ultra-low attachment plates cells were treated with GSK J4 for indicated dose for consecutive 5 days. The fresh treatment was added every 48 hours, following completion of treatment, media was aspirated and cells were washed with cold PBS (pH 7.4) and pelleted in 15ml falcon tubes. Ice-cold lysis buffer was added to the pellet. The composition of lysis buffer was 50 mM Tris−HCl, 150 mM NaCl, 1 mM ethyleneglycol-bis(aminoethylether)-tetraacetic acid, 1 mM ethylenediaminetetraacetic acid, 20 mM NaF, 100 mM Na_3VO_4, 0.5% NP-40, 1% Triton X-100, 1 mM phenylmethylsulfonyl fluoride, pH 7.4 with freshly added protease inhibitor cocktail (Protease Inhibitor Cocktail Set III, Calbiochem, La Jolla, CA). Then cells were passed through needle of the syringe to break up the cell aggregates. The lysate was cleared by centrifugation at $14000g$ for 30 min at 4°C and the supernatant (nuclear lysate) was used or immediately stored at −80°C. For western blotting 4-12% poly acrylamide gels were used to resolve 30μg of protein, transferred on to a nitrocellulose membrane, probed with appropriate monoclonal primary antibodies and detected by chemiluminescence after incubation with specific secondary antibodies [19].

Flow cytometry analysis

HeLa, HCT116 and 22RΩ1 cells were grown in ultra-low attachment plate for six days with and without treatment of GSK J4 and matrix detached cells were washed two times in ice-cold PBS and resuspended in 100 μl of staining solution (5 μl PE-conjugated anti-CD 73 (BD Bioscience), CD 133 (Miltenyibiotec -130-090-853) and FITC conjugated anti-CD 105(BD Bioscience- 56143), and anti-CD44(Miltenyibiotec -130-098-210), 1% FBS, in 1X PBS and incubated at room temperature under the dark condition for 2 hours. Then, cells were washed three times in wash buffer (1%FBS in 1X PBS) and then analyzed by Guava Easy-Cyte flow cytometer. For all assays, 10,000 cells were taken for measurement and also for analysis. For each plot 1000 cells were displayed.

Immunofluorescence

Immunofluorescence assay, cells were grown in ultra-low attachment plates for six days with and without treatment of GSK J4. Then, cells were collected and washed two times with ice-cold PBS ad cells were stained with staining solution containing (5 μl PE-conjugated anti-CD 73, CD 133 and FITC anti-CD 105, and anti-CD44), 1% FBS, in 1X PBS and incubated at room temperature in dark for 2 hours. Then cells were washed two times in ice-cold PBS and counterstained with DAPI. Stained cells were imaged with the EVOS FL cell imaging system (Thermo Fisher Scientific, USA).

Apoptosis assay

The apoptotic cells were detected by using Annexin V-FITC and propidium iodide. The cells were grown in an ultra-low attachment plate for 6 days with and without treatment with GSK J4. After treatment, spheroids were harvested and washed with PBS (ice cold) three times. The spheroids were breakdown by multiple pipetting and resuspended in 100 μL 1X binding buffer and 10 μL Annexin V-FITC and 5 μL PI.

After incubation for 20 min in RT (dark condition). The cells were analyzed by flow The Guava® easyCyte 5 Flow Cytometer and the percentage of cells went apoptosis was calculated [20].

CHIP assay and PCR

The CHIP experiment was performed using Abcam (ab185913) chip kit. The protocol was followed as per standard guidelines of manual with minor modification. The spheroids (ECM detached), ECM attached cells and ECM detached cells were harvested and washed with ice with 3mL PBS and cells were resuspended in 1% formaldehyde in DMEM and incubate at RT for 10 min with the minor rocking platform and 300 μL of 1.25M glycin are added for crosslinking and washed with ice-cold PBS. The pellet was resuspended in 300 μL lysis buffer and chromatin was sheared using a water bath sonicator (15 cycles on and 15 cycles off for 20 min). Three micrograms of sheared chromatin were taken to the well coated with KDM6B antibodies, input (negative control) along with nonimmune IgG and incubated for overnight at 4°C. The unbounded chromatins were removed and washed with wash buffer and DNA was released using DNA release buffer and incubated at 60°C for 45 minutes in a water bath and subsequently, the solution was transferred to PCR tubes and heated for 95°C for 15 min at thermocycler. The DNA was purified by using the column provided in the kit. The PCR was performed by using the targeted primers (Table-2) of specific genes.

KDM6 histone demethylase activity assay

Histone H3K27 demethylase KDM6A/B activity was measured by Abcam- KDM6A/B activity quantification kit (ab156910). The protocol was performed based on Kit guideline 15μg of nuclear extract was used. Nuclear protein was extracted without using detergent. The ECM detached cells with and without treatment of GSK J4 and ECM attached cells 2×10^6. Wash with Ice cold PBS three times in 500g for 10 min in 500 μL of lysis buffer 10 mM HEPES, pH 7.9, with 1.5 mM MgCl 2 and 10 mM KCl (add 5μL of 0.1M DTT and 5μL of protease inhibitor cocktail) incubate for 15 min ice. Spin and remove the supernatant and pellet was resuspended in 200 μL of lysis buffer and give five gentle strokes using a glass homogenizer. Spin 20 min at 12,000 g. Remove the cytosolic fraction(supernatant) and add 150 μL of nuclear extraction buffere20 mM HEPES, pH 7.9, with 1.5 mM MgCl 2 , 0.42 M NaCl, 0.2 mM EDTA, 25% (v/v) Glycerol with add 1.5μL of 0.1M DTT and 1.5μL of protease inhibitor cocktail. Incubate in ice for 30 min with a gentle shake for every 2 min and spin at 21000 g for 10 min and save supernatant (Nuclear protein).

H3K27 methyltransferase activity assay

The H3K27 specific methyltransferase activity was performed by using a commercially available kit from Abcam (H3K27 methylation Assay Kit (Colorimetric) # ab113463). The assay kit was capable of measuring activity or inhibition of H3K27 mono/di/tri subtypes and required cellular nuclear extracts. Briefly, equal amounts of protein samples were added in each independent experiment, however, overall protein concentration range from 100 to 300 ng. H3K27 modifications were calculated according to

manufacturer's instructions, which also accounts for protein amounts and the final values for each modification were presented as the percentage over untreated control.

Gene expression correlation analysis

For the correlation analysis of gene expression among KDM6B, SOX2, CD44, and HIF1α, gene expression profile was taken from two different studies. (i) Metastatic melanoma sample was taken from Hugo et al. 2016 (PMID: 26997480). The study provided the normalized gene expression data in FPKM value from 27 samples. (ii) Metastatic breast cancer data of Metastatic Breast Cancer Project (www.mbcproject.org). The study provided the normalized gene expression data in RSEM values from 146 samples. The normalized expression values were transformed into log2 (x+0.1), and then the Pearson correlation coefficient was measured with the ggpubr package of R version 3.5.2.

Statistical analysis

Data were analyzed using GraphPad Prism (version 5; GraphPad Software). Two-tailed, unpaired *t* test was used. Data points in graphs represent mean ± SD, and *p* values < 0.05 were considered significant.

Results

Matrix detachment of cancer cells induces histone H3K27me3 demthylase KDM6B expression and activity

Based on the well-established protocols for culturing cancer cells in ECM detached conditions, different cell lines namely HeLa, HCT116 and 22Rυ1 were cultured in ultra-low attachment plates for short i.e. 30 min, 6 hours and 24 hours and long i.e. 6days time points. After establishing the ECM detachment cultures, we firstly evaluated the expression of hypoxia markers i.e. HIF1α, HIF2α and its target gene VEGF, results showed dramatic induction of all the genes tested in ECM detached condition when compared to attached cells, clearly suggesting hypoxia in ECM detached condition (Fig. 1a). Next, we measured the expression of hypoxia regulated histone demethylases in ECM detachment condition of different cancer cell types. Quantitative gene transcript data of early time points (from 30 min to 24 hour) showed statistically significant induction of typical hypoxia regulated histone demethylases like JARID1A, JARID2, JMJD1A and KDM6B in all the three cancer cell types grown in ECM detached conditions (Fig. 1b). Further, we decided to look into the expression pattern of the above tested histone demethylases in long term ECM detachment condition i.e. 6 days. One histone demethylase namely KDM6B stand out as its expression was consistently upregulated in all three cell lines during ECM detached condition when compared with attached (Fig. 1c).

Since KDM6B, a H3K27 demethylase was the most consistently upregulated at all time points in all cell types, we decided to focus our further work on KDM6B. Next, we performed quantitative activity assay for KDM6B demethylase and found a statistically significant increase in the KDM6B demethylase activity in HeLa and HCT116 cell lines in ECM detached condition when compared with attached condition. Further,

in 22Ru1 we noticed an insignificant increase in ECM detached condition when compared with attached condition (Fig. 1d). Based on the above data it is clear that ECM detachment of cancer induces the hypoxic response and expression and activity of KDM6B, removes the repressive H3K27me3 mark across the genome and thereby facilitates global transcription.

KDM6B regulates SOX2 and CD44 stemness marker genes in matrix detached condition.

Matrix detachment of cancer cells often present induced expression stemness genes, therefore we quantified the expression of genes related to stemness like ALDH1, Sox-2, Sox-9 and CD44 and found significantly increased levels of these stemness genes in all ECM detached cancer cell lines when compared to their attached counterparts (Fig. 2a). We further validated the stemness by measuring the surface protein marker of stemness like CD44, CD133 and mesenchymal markers namely CD73 and CD105 by flow cytometry. As expected, we observed statistically significant up-regulation of surface stemness and mesenchymal markers in all ECM detached cancer cells when compared to attached cells. Our data clearly represents that ECM detachment induces the stemness (Fig. 2b).

To investigate the role of KDM6B demethylase in the transcriptional regulation of stemness genes, we treated all the ECM detached cancer cell types with GSK J4 (a H3K27 demethylase specific inhibitor) for a total period of 5 days after the initial 24 hours of detachment. GSK J4 treatment significantly reduces the KDM6 activity in all cell lines, along with GSK J4 treatment induces global H3K27me2/3 methylation (Fig. 2C, 2G and 2H). Further data showed that GSK J4 treatment significantly reduces the transcript levels of Sox2, Sox9, and CD44 genes in ECM detached cancer cells when compared to the untreated control (Fig. 2d). Next, we assess the impact of GSK J4 treatment on expression of stemness related surface proteins by using both flow cytometry and immunofluorescence and found that GSK J4 significantly reduced the expression of CD44, CD133, CD70 but not CD105 in ECM detached cells when compared to untreated (Fig. 2e; supplementary Fig. 1).

Since KDM6B binds to promoters of its target genes to regulate their expression, we next aimed to investigate whether KDM6B binds to the promoters of target stemness genes. For this, we performed Chip-RT PCR assay and found significant enrichment of KDM6B on promoters of Sox2 and CD44 but not on Sox9 in ECM detached cancer cells. Further, GSK J4 treatment significantly reduces the occupancy of KDM6B on promoters of both Sox2 and CD44 suggesting the KDM6B driven regulation of these stemness genes in ECM detached cancer cells (Fig. 2f).

In a feedback loop, KDM6B regulates HIF-1α expression in matrix detached condition

Hypoxia driven regulation of histone demethylases expression and activity is a well-established phenomenon. However, in opposite to this, recent studies have shown that various histone methyltransferases like SET7/9, G9a and GLP can methylate HIF1A and thereby regulate and represses its expression. This prompted us to investigate whether induction in KDM6B activity during ECM detachment might positively regulate the hypoxia related transcription factors HIF1α and HIF2α expression and reduction of KDM6B activity (using GSKJ4) will negatively regulate its expression. To

explore this, we treated cells with GSK J4 in two conditions i.e. ECM detached and DMOG (a hypoxic mimic) and found that the GSK J4 was able to reduce the expression of HIF1α, HIF2α and its target gene VEGF, suggesting KDM6B mediated transcriptional regulation of hypoxic transcription factors (Fig. 3a). Next, we set to identify that whether KDM6B occupies the promoter of hypoxic transcription factors and regulate their expression. Results showed a clear enrichment of KDM6B on HIF1α promoter and a subsequent reduction in the enrichment by GSK J4, further confirming the transcriptional regulation of HIF1α in matrix detached condition (Fig. 3b). We further strengthened our initial observation by finding that hypoxia induces expression of KDM6B by using DMOG (1mM for 24 hours; Fig. 3c).

Overall, we found that hypoxia induces KDM6B expression activity and reciprocally KDM6B binds to the promoter and positively regulates the expression of HIF1α, creating a positive feedback loop between hypoxia (HIF1α) and KDM6B.

Clinical Mrna Expression Association Of KDM6B And HIF1α

Based on our results that KDM6B transcriptionally regulate the expression of HIF1α, we next investigated the positive association between KDM6B and HIF1α in clinical samples using TCGA datasets. We found a positive association between KDM6B and HIF1α in various cancer types. In metastatic melanoma and breast cancer samples, a significantly high positive correlation was observed between KDM6B and HIF1α (R = 0.45, p-value = 0.018; R = 0.26, p-value = 0.0014) (Fig. 4a & b). Similarly, we found a significant positive association between HIF1α and SOX2 (R = 0.49, p-value = 0.0089) along with CD44 and SOX2 (R = 0.39, p-value = 0.045) in melanoma cancers. In addition to this we also found that metastatic breast samples, a significantly high positive correlation was observed between CD44 and HIF1α (R = 0.24, p-value = 0.0031) (supplementary Fig. 2).

Targeting KDM6B reduces sphere-forming capabilities and induces apoptosis of cancer cells during matrix detachment

Matrix detachment of cancer cells tends to form spheroids. We therefore, tested whether inhibiting KDM6B will affect spheroid formation and size. We treated spheroids of HeLa, HCT116 and 22Rυ1 that formed during matrix detachment with GSK J4. Results showed that GSK J4 significantly reduced the size of spheroids of all cancer cell lines tested when compared to untreated respectively (Fig. 5a). Next, we measure the percentage of cell death that might have occurred in ECM detached cancer cells during GSK J4 treatment. As expected, GSK J4 significantly induces apoptosis in all the ECM detached cancer cells. Among them 22Rυ1showed the maximum percentage of apoptotic cells (57.7%) when compared with HeLa (34.4%) and HCT116 (22.8%) (Fig. 5b). Overall, we observed that GSK J4 treatment reduces the sphere forming capacity and invokes apoptosis in ECM detached cancer cells.

Discussion

Matrix detachment has been shown to have increased expression of hypoxia and stemness markers, however, the mechanism regulating these markers are not well explored yet. In the current work, we found

that (1) matrix detachment induces expression of KDM6B, a histone H3K27me2/3 demethylase in all cell types tested. (2) Inhibition of KDM6B activity reduces the expression of two major cancer stem cell (CSCs) markers namely SOX-2 and CD44, found to be highly expressed during matrix detachment. (3) Mechanistically, KDM6B nuclear localization is increased and KDM6B occupies the promoter region of these CSCs regulators and thereby regulate their expression. (4) We also noticed that HIF1α was transcriptionally regulated by KDM6B in ECM detached cancer cells. (5) Finally, we observed a positive association between KDM6B, HIF1α and SOX2 in various cancer types. Overall, we found, that matrix detachment modulates epigenome, induces KDM6B that positively regulate expression of SOX2, CD44 and HIF1α to regulate survival and stemness of cancer cells.

Hypoxia has been recently reported to be associated with matrix detachment of cancer cells and can regulate the metabolism of matrix detach cancer cells [17]. Our results are in clear agreement with this study as we also found a clear induction in the expression of HIF and its target genes. Hypoxia, regulates global transcription by multiple ways, and regulation of expression and activity of histone demethylases is one of them [21]. Therefore, we target to explore the expression pattern of hypoxia regulated histone demethylases in matrix detached cancer cells. Results of our study showed significant and consistent upregulation of KDM6B in all cell lines at all the time points tested. KDM6B plays a crucial and dual role in cancer initiation and progression through binding to promoters of oncogenes or suppressor genes. KDM6B was found to be associated with aggressiveness and enhanced migratory properties of various cancer types [22, 23]. Further, KDM6B was shown to regulate epithelial to mesenchymal (EMT) conversion of cancer cells by regulating the expression of essential transcription factor of EMT process [24, 25]. This clearly suggest KDM6B as a key regulator of metastasis in different cancer types. Our findings that KDM6B expression and activity is increased and essential for spheroids maintenance during matrix detachment aligns well with these previous studies.

Various histone methylases including KDM6B are known to regulate stemness of both normal and cancer stem cells [21, 26–29]. In this study we found that blocking KDM6B activity showed dramatic reduction in the expression of stemness marker genes mainly SOX2, SOX9 and CD44, suggesting their epigenetic regulation in matrix detached condition. The post translational modifications of SOX2 are shown to regulates its protein stability and transcriptional activity. AKT mediated phosphorylation at Thr118 promotes the transcriptional activity of SOX2 in ESCs [30]. Further, [31] showed that Set7 methylates SOX2 at K119, which inhibits Sox2 transcriptional activity and induces Sox2 ubiquitination and degradation. In our study we found that KDM6B occupies SOX2 promoter in matrix detached condition, probably reduces the repressive H3K27me3 from its promoter and increases its expression. A previous study by [32] had shown that GSK J4 treatment reduces expression of stemness genes i.e. SOX2, Nanog and OCT4 in breast cancer stem cells, however, they did not present a direct evidence that KDM6B occupies the promoter of these genes in cancer cells.

CD44 is prominent and well-established marker of stem cells and its expression can be regulated at epigenetic levels. DNA methylation of CD44 promoter by DNA methyltransferases (DNMTs), MBD1, MBD2 and MeCP2 is well reported [33, 34]. In our work we found that KDM6B occupies the promoter of CD44

during matrix detachment of cancer cells. Our finding of KDM6B mediated transcriptional regulation of CD44 is in clear agreement with [35, 36] who showed CD44 as a bonafide target of KDM6B in immune and leukemic cells. However, we strongly believe, this is the first report to show epigenetic regulation of CD44 by KDM6B in various solid cancer types. Furthermore, positive correlation of gene expression from two different metastatic cancer data suggesting the involvement of KDM6B in regulating HIF1α, SOX2, CD44, further indicates the stemness regulatory function of KDM6B in different cancer types.

During the course of our study we also noticed a surprised finding that treatment of GSK J4 reduces the mRNA levels of HIF1α, HIF2α and its target gene VEGF, hinting KDM6B mediated regulation of their expression. We checked and found that KDM6B occupies the promoter of HIF1α and regulates its expression in matrix detached cancer cells. We believe this might a feed forward loop as induction of hypoxia or knockdown of HIF1α increase and decreases the KDM6B expression. Similarly, KDM6B inhibition also reduces the expression of HIF1α, however we were not able to confirm whether HIF1α promoter is occupied by H3K27me3 and its level were decreased with simultaneous increase in KDM6B activity and occupancy of HIF1α promoter during matrix attachment. Some recent studies have shown that HIF1α expression can be regulated by methylation [37, 38]. The regulation of HIF1α expression by H3K37me3 and KDM6B needs further work in order to confirm its regulation through this axis.

In conclusion, our data suggest that the rapid and sustained upregulation of KDM6B following matrix detachment is necessary for SOX2 and CD44-mediated stemness to enhance anchorage-independent survival of variety of cancer cells. Additional consequences of the context-specific increase and regulation of HIF1α by KDM6B might likely to further aid in survival in response to changing nutrient microenvironments. Our study highlights an important role of KDM6B in cancer and has important implications for future targeting of this protein for anticancer therapies.

Declarations

Conflict of interest

The authors declare no conflict of interest.

Ethics approval: Not applicable

Consent to Participate: Not applicable

Consent to Publish: Not applicable

Availability of data and materials: Not applicable

Author's Contributions

MRM, MIK and HC designed and performed the experiments and analyzed the data. BA and MIK and FZ carried out the bioinformatic analysis. MIK and MZ and HC designed the study and supervised all aspects

of data collection. MIK, MRM and FA wrote the manuscript. All authors read and approved the final manuscript.

Code availability: Not applicable

References

1. Simpson CD, Anyiwe K, Schimmer AD (2008) Anoikis resistance and tumor metastasis. Cancer Lett. 18;272(2):177-85. doi: 10.1016/j.canlet.2008.05.029

2. Chaffer CL, Weinberg RA (2011) A perspective on cancer cell metastasis. Science. 25;331(6024):1559-64. doi: 10.1126/science.1203543.

3. Buchheit CL, Weigel KJ, Schafer ZT (2014) Cancer cell survival during detachment from the ECM: multiple barriers to tumour progression. Nat Rev Cancer.14(9):632-41. doi: 10.1038/nrc3789.

4. Paoli P, Giannoni E, Chiarugi P (2013) Anoikis molecular pathways and its role in cancer progression. Biochim Biophys Acta. 1833(12):3481-3498. doi: 10.1016/j.bbamcr.2013.06.026.

5. Polyak K, Weinberg RA (2009) Transitions between epithelial and mesenchymal states: acquisition of malignant and stem cell traits. Nat Rev Cancer.9(4):265-73. doi: 10.1038/nrc2620.

6. Kim YN, Koo KH, Sung JY, Yun UJ, Kim H (2012) Anoikis resistance: an essential prerequisite for tumor metastasis. Int J Cell Biol. 2012:306879. doi: 10.1155/2012/306879.

7. Labuschagne CF, Cheung EC, Blagih J, Domart MC, Vousden KH (2019) Cell Clustering Promotes a Metabolic Switch that Supports Metastatic Colonization. Cell Metab.30(4):720-734.e5. doi: 10.1016/j.cmet.2019.07.014.

8. Aceto N, Bardia A, Miyamoto DT, Donaldson MC, Wittner BS, Spencer JA, Yu M, Pely A, Engstrom A, Zhu H, Brannigan BW, Kapur R, Stott SL, Shioda T, Ramaswamy S, Ting DT, Lin CP, Toner M, Haber DA, Maheswaran S (2014) Circulating tumor cell clusters are oligoclonal precursors of breast cancer metastasis. Cell.158(5):1110-1122. doi: 10.1016/j.cell.2014.07.013.

9. Heerboth S, Housman G, Leary M, Longacre M, Byler S, Lapinska K, Willbanks A, Sarkar S (2015) EMT and tumor metastasis. Clin Transl Med.26;4:6. doi: 10.1186/s40169-015-0048-3.

10. Gkountela S, Castro-Giner F, Szczerba BM, Vetter M, Landin J, Scherrer R, Krol I, Scheidmann MC, Beisel C, Stirnimann CU, Kurzeder C, Heinzelmann-Schwarz V, Rochlitz C, Weber WP, Aceto N (2019) Circulating Tumor Cell Clustering Shapes DNA Methylation to Enable Metastasis Seeding. Cell. 176(1-2):98-112.e14. doi: 10.1016/j.cell.2018.11.046.

11. Pollard PJ, Loenarz C, Mole DR, McDonough MA, Gleadle JM, Schofield CJ, Ratcliffe PJ (2008) Regulation of Jumonji-domain-containing histone demethylases by hypoxia-inducible factor (HIF)-1alpha. Biochem J.416(3):387-94. doi: 10.1042/BJ20081238.

12. Xia X, Lemieux ME, Li W, Carroll JS, Brown M, Liu XS, Kung AL (2009) Integrative analysis of HIF binding and transactivation reveals its role in maintaining histone methylation homeostasis. Proc Natl Acad Sci 106(11):4260-5. doi: 10.1073/pnas.0810067106.

13. Lee HY, Choi K, Oh H, Park YK, Park H (2014) HIF-1-dependent induction of Jumonji domain-containing protein (JMJD) 3 under hypoxic conditions. Mol Cells. 37(1):43-50. doi: 10.14348/molcells.2014.2250.

14. Choudhry H, Harris AL (2018) Advances in Hypoxia-Inducible Factor Biology. Cell Metab.;27(2):281-298. doi: 10.1016/j.cmet.2017.10.005.

15. Chakraborty AA, Laukka T, Myllykoski M, Ringel AE, Booker MA, Tolstorukov MY, Meng YJ, Meier SR, Jennings RB, Creech AL, Herbert ZT, McBrayer SK, Olenchock BA, Jaffe JD, Haigis MC, Beroukhim R, Signoretti S, Koivunen P, Kaelin WG Jr (2019) Histone demethylase KDM6A directly senses oxygen to control chromatin and cell fate. Science.363(6432):1217-1222. doi: 10.1126/science.aaw1026.

16. Batie M, Frost J, Frost M, Wilson JW, Schofield P, Rocha S (2019) Hypoxia induces rapid changes to histone methylation and reprograms chromatin. Science. 363(6432):1222-1226. doi: 10.1126/science.aau5870.

17. Labuschagne CF, Cheung EC, Blagih J, Domart MC, Vousden KH (2019) Cell Clustering Promotes a Metabolic Switch that Supports Metastatic Colonization. Cell Metab.30(4):720-734.e5. doi: 10.1016/j.cmet.2019.07.014.

18. Endo H, Owada S, Inagaki Y, Shida Y, Tatemichi M (2020) Metabolic reprogramming sustains cancer cell survival following extracellular matrix detachment. Redox Biol. 2020 Sep;36:101643. doi: 10.1016/j.redox.2020.101643.

19. Shait Mohammed MR, Krishnan S, Amrathlal RS, Jayapal JM, Namperumalsamy VP, Prajna L, Kuppamuthu D (2020) Local Activation of the Alternative Pathway of Complement System in Mycotic Keratitis Patient Tear. Front Cell Infect Microbiol. 2020;10:205.. doi:10.3389/fcimb.2020.00205

20. AlGhamdi, A.A.; Mohammed, M.R.S.; Zamzami, M.A.; Al-Malki, A.L.; Qari, M.H.; Khan, M.I.; Choudhry, H (2020) Untargeted Metabolomics Identifies Key Metabolic Pathways Altered by Thymoquinone in Leukemic Cancer Cells. *Nutrients*2020, *12*, 1792.

21. Shmakova A, Batie M, Druker J, Rocha S (2014) Chromatin and oxygen sensing in the context of JmjC histone demethylases. Biochem J. 2014 Sep 15;462(3):385-95. doi: 10.1042/BJ20140754.

22. Burchfield JS, Li Q, Wang HY, Wang RF (2015) JMJD3 as an epigenetic regulator in development and disease. Int J Biochem Cell Biol. 67:148-57. doi: 10.1016/j.biocel.2015.07.006.

23. Fu C, Li Q, Zou J, Xing C, Luo M, Yin B, Chu J, Yu J, Liu X, Wang HY, Wang RF(2019). JMJD3 regulates CD4 T cell trafficking by targeting actin cytoskeleton regulatory gene Pdlim4. J Clin Invest.129(11):4745-4757. doi: 10.1172/JCI128293.

24. Ramadoss S, Chen X, Wang CY (2012) Histone demethylase KDM6B promotes epithelial-mesenchymal transition. J Biol Chem. 2012 Dec 28;287(53):44508-17. doi: 10.1074/jbc.M112.424903.

25. Liu X, Li C, Zhang R, Xiao W, Niu X, Ye X, Li Z, Guo Y, Tan J, Li Y(2018) The EZH2- H3K27me3-DNMT1 complex orchestrates epigenetic silencing of the wwc1 gene, a Hippo/YAP pathway upstream effector, in breast cancer epithelial cells. Cell Signal.51:243-256. doi: 10.1016/j.cellsig.2018.08.011.

26. Sakaki H, Okada M, Kuramoto K, Takeda H, Watarai H, Suzuki S, Seino S, Seino M, Ohta T, Nagase S, Kurachi H, Kitanaka C (2015) GSKJ4, A Selective Jumonji H3K27 Demethylase Inhibitor, Effectively Targets Ovarian Cancer Stem Cells. Anticancer Res. 35(12):6607-14.

27. Akiyama T, Wakabayashi S, Soma A, Sato S, Nakatake Y, Oda M, Murakami M, Sakota M, Chikazawa-Nohtomi N, Ko SB, Ko MS(2016) Transient ectopic expression of the histone demethylase JMJD3 accelerates the differentiation of human pluripotent stem cells. Development. 143(20):3674-3685. doi: 10.1242/dev.139360.

28. Jeong CH, Cho YY, Kim MO, Kim SH, Cho EJ, Lee SY, Jeon YJ, Lee KY, Yao K, Keum YS, Bode AM, Dong Z (2010) Phosphorylation of Sox2 cooperates in reprogramming to pluripotent stem cells. Stem Cells.28(12):2141-50. doi: 10.1002/stem.540.

29. Tang B, Qi G, Tang F, Yuan S, Wang Z, Liang X, Li B, Yu S, Liu J, Huang Q, Wei Y, Zhai R, Lei B, Yu H, Tomlinson S, He S (2016) Aberrant JMJD3 Expression Upregulates Slug to Promote Migration, Invasion, and Stem Cell-Like Behaviors in Hepatocellular Carcinoma. Cancer Res.76(22):6520-6532. doi: 10.1158/0008-5472.CAN-15-3029.

30. Mallaney C, Ostrander EL, Celik H, Kramer AC, Martens A, Kothari A, Koh WK, Haussler E, Iwamori N, Gontarz P, Zhang B, Challen GA (2019) Kdm6b regulates context-dependent hematopoietic stem cell self-renewal and leukemogenesis. Leukemia. 33(10):2506-2521. doi: 10.1038/s41375-019-0462-4.

31. Fang L, Zhang L, Wei W, Jin X, Wang P, Tong Y, Li J, Du JX, Wong J (2014) A methylation-phosphorylation switch determines Sox2 stability and function in ESC maintenance or differentiation. Mol Cell.55(4):537-51. doi: 10.1016/j.molcel.2014.06.018.

32. Yan N, Xu L, Wu X, Zhang L, Fei X, Cao Y, Zhang F (2017) GSKJ4, an H3K27me3 demethylase inhibitor, effectively suppresses the breast cancer stem cells. Exp Cell Res.359(2):405-414. doi: 10.1016/j.yexcr.2017.08.024.

33. Müller I, Wischnewski F, Pantel K, Schwarzenbach H (2010) Promoter- and cell-specific epigenetic regulation of CD44, Cyclin D2, GLIPR1 and PTEN by methyl-CpG binding proteins and histone modifications. BMC Cancer.;10:297. doi: 10.1186/1471-2407-10-297.

34. Eberth S, Schneider B, Rosenwald A, Hartmann EM, Romani J, Zaborski M, Siebert R, Drexler HG, Quentmeier H (2010) Epigenetic regulation of CD44 in Hodgkin and non-Hodgkin lymphoma. BMC Cancer.10:517. doi: 10.1186/1471-2407-10-517

35. Itoh Y, Golden LC, Itoh N, Matsukawa MA, Ren E, Tse V, Arnold AP, Voskuhl RR (2019) The X-linked histone demethylase Kdm6a in CD4+ T lymphocytes modulates autoimmunity. J Clin Invest.129(9):3852-3863. doi: 10.1172/JCI126250.

36. Li Q, Zou J, Wang M, Ding X, Chepelev I, Zhou X, Zhao W, Wei G, Cui J, Zhao K, Wang HY, Wang RF (2014) Critical role of histone demethylase Jmjd3 in the regulation of CD4+ T-cell differentiation. Nat Commun. 5:5780. doi: 10.1038/ncomms6780.

37. Kim Y, Nam HJ, Lee J, Park DY, Kim C, Yu YS, Kim D, Park SW, Bhin J, Hwang D, Lee H, Koh GY, Baek SH (2016) Methylation-dependent regulation of HIF-1α stability restricts retinal and tumour angiogenesis. Nat Commun. 7:10347. doi: 10.1038/ncomms10347.

38. Bao L, Chen Y, Lai HT, Wu SY, Wang JE, Hatanpaa KJ, Raisanen JM, Fontenot M, Lega B, Chiang CM, Semenza GL, Wang Y, Luo W (2018) Methylation of hypoxia-inducible factor (HIF)-1α by G9a/GLP inhibits HIF-1 transcriptional activity and cell migration. Nucleic Acids Res. 46(13):6576-6591. doi: 10.1093/nar/gky449.

Tables

Table 1: List of primers for real time PCR

hJARID1A	5'-TGTGTTGAGCCAGCGTATGG-3'	5'-CCACCCGGTTAAAAGCAGACT-3'
hJARID2	5'-TGTTCACAACGGGCATGTTT-3'	5'-TTGTGTTTTTGAACAGGTTCCTTCT-3'
hKDM3A	5'-GTGGTTTTCAGCAACCGTTATAAA-3'	5'-CAGTGACGGATCAACAATTTTCA-3'
hKDM3B	5'-TGCCCTTGTATCAGTCGACAGA-3'	5'GCACTAGGGTTTATGCTAGGAAGCT-3'
hKDM4A	5'-TGCAGATGTGAATGGTACCCTCTA-3'	5'-CACCAAGTCCAGGATTGTTCTCA-3'
hKDM4B	5'-GGCCTCTTCACGCAGTACAATAT-3'	5'-CCAGTATTTGCGTTCAAGGTCAT-3'
hKDM4C	5'-GAATGCTGTCTCTGCAATTTGAGA-3'	5'-CAACGGCGCACATGACAT-3'
hKDM6B	5'-CGGAGACACGGGTGATGATT-3'	5'-CAGTCCTTTCACAGCCAATTCC-3'
hSOX2	5'- TGATCATGTCCCGGAGGT-3'	5'- CATGGGTTCGGTGGTCAAG-3'
hSOX9	5'- TCTACTCCACCTTCACCTACAT-3'	5'-CTGTGTGTAGACGGGTTGTT-3'
hOct-4	5'- GGAGGAAGCTGACAATGAAA-3'	5'- GGAGGAAGCTGACAATGAAA-3'
hCD44	5'- CAGCACTTCAGGAGGTTACAT-3'	5'- GTAGCAGGGATTCTGTCTGTG-3'
LinVEGFA	5'-GCCTCCGAAACCATGAACTTT-3'	5'-CCATGAACTTCACCACTTCGT-3'
Lin HIF 2α	5'-CTGAACGTCTCAAAGGGCCA-3'	5'-CCTTCCTCCTCTCCGAGCTA-3'
Lin HIF 1α	5'-ATGCTTTAACTTTGCTGGCCC-3'	5'-TCTGTGTCGTTGCTGCCAAA-3'

Table 1: List of primers for CHIP-PCR

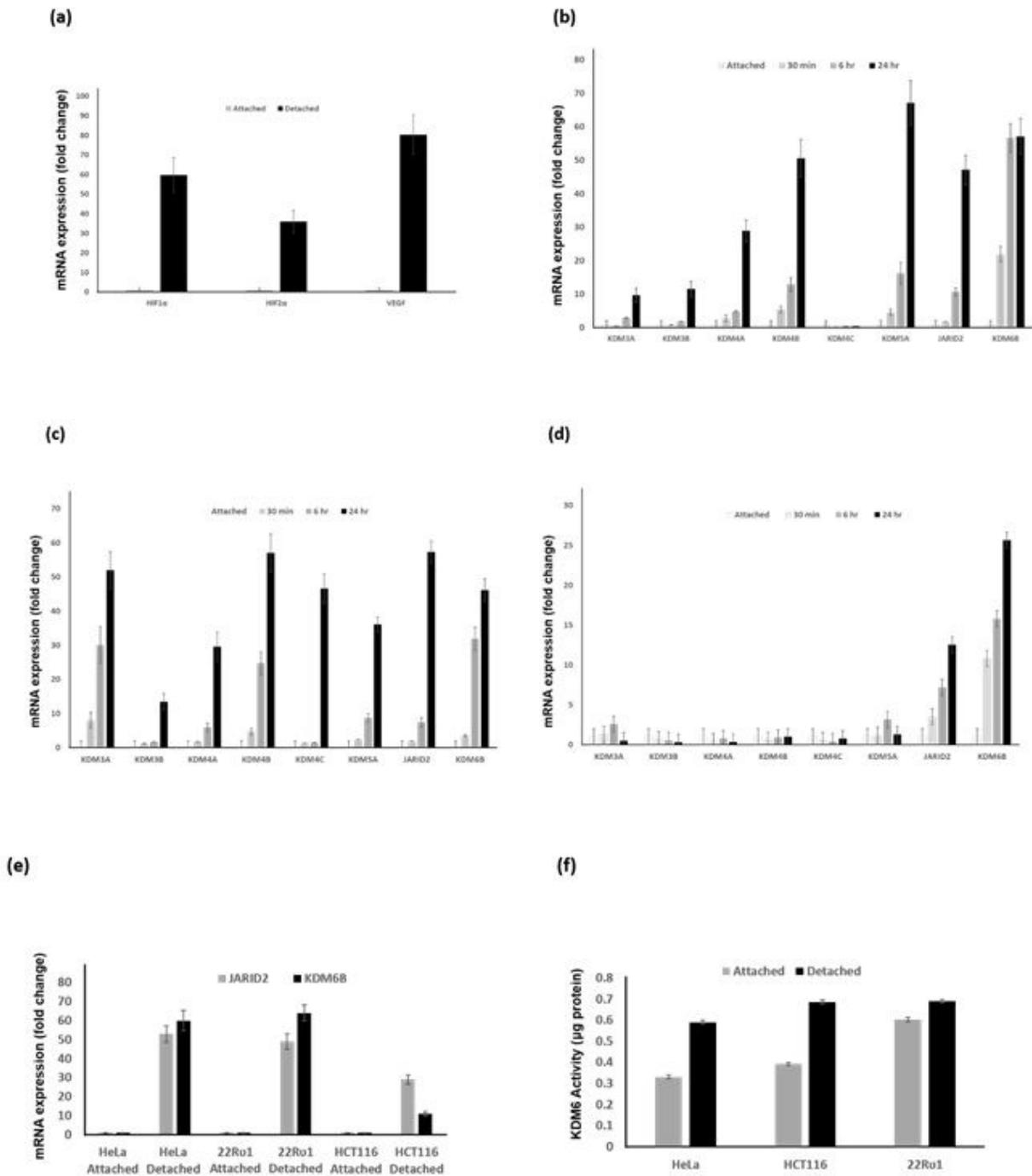| Chip-CD44	5'- CTGGCAGCCCCGATTATT -3'	5- AGCGAGCGAAGGACACAC-3'
Chip-Sox9	5'- GCTCTAAGCATTTCGTGTAA -3'	5'- TACGAAACACCTGAAGGG-3'
Chip-SOX2	5'- CGACAACAAGAGAAACAAAAC-3'	5'- CCAGCAAGGCCCGGGTTA-3'
Chip-HIF1α	5' GAAGTTTACAGCAACAGGAG-3'	5'- TTACAACGGGGTCTTTCCTTAC-3'

Figures

Figure 1

Matrix detachment induces hypoxia regulated KDM6B expression and activity. a. Matrix detachment induces expression of HIF1α, HIF2 α and target gene VEGF in HeLa cell lines. b-d. Expression of various hypoxia regulated histone demethylases in HeLa, HCT116 and 22Rʋ1 cell lines during matrix detachment at shorter time points (30 mins, 6 and 24 hours). e. Expression of JARID2 and KDM6B in HeLa, HCT116 and 22Rʋ1 cell lines during matrix detachment at 6 days. The values were normalized with housekeeping

gene RPLP0 and further gene expression values were calculated. f. KDM6 demethylase activity was measured in nuclear extract of HeLa, HCT116 and 22Rʋ1 cells grown in matrix detached conditions.
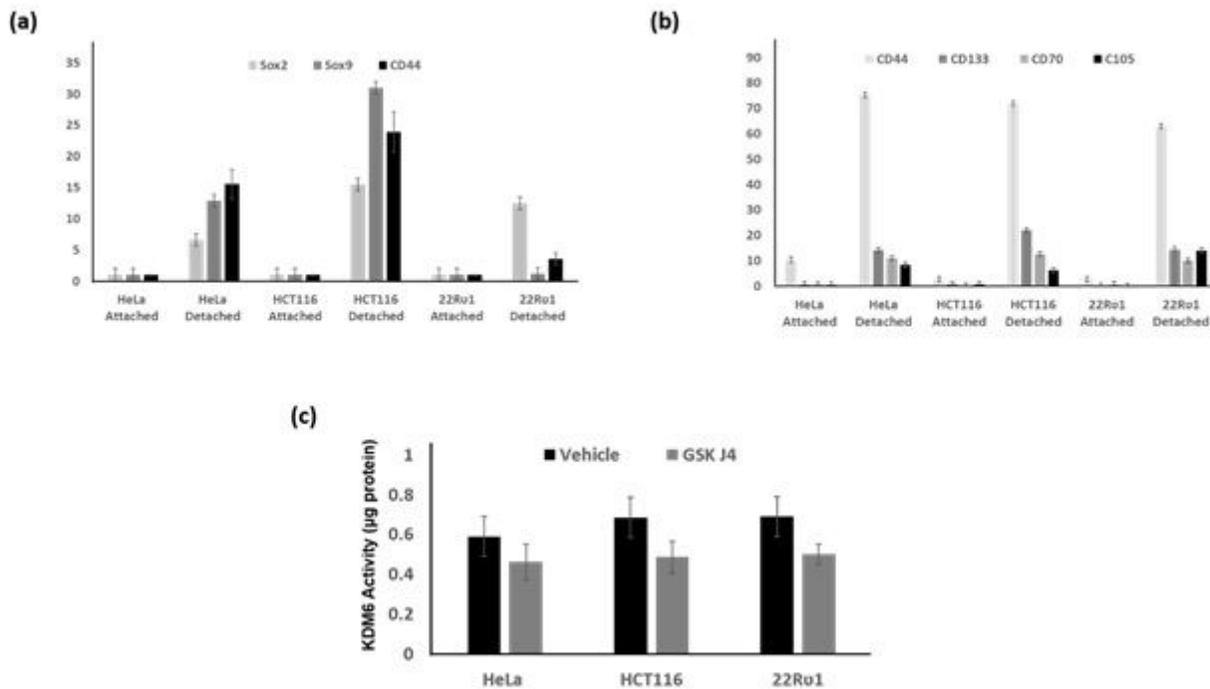

Figure 2

Matrix detachment induces expression of stemness markers that are repressed by KDM6B specific inhibitor. a. mRNA expression of various stemness related genes (SOX2, SOX9 and CD44) in HeLa, HCT116 and 22Rʋ1 cell lines during matrix detachment at 6 days. The values were normalized with housekeeping gene RPLP0 and further gene expression values were calculated. b. Flow cytometry-based expression of various surface markers of stemness in HeLa, HCT116 and 22Rʋ1 cell lines during matrix detachment at 6 days. c. Impact of GSK J4 (7.5µM) a specific inhibitor of KDM6 histone demethylases on KDM6 activity in nuclear extracts of HeLa, HCT116 and 22Rʋ1 cell lines during matrix detachment at 6 days. d. Impact of GSK J4 (7.5µM) on mRNA expression of various stemness related genes (SOX2, SOX9 and CD44) in HeLa, HCT116 and 22Rʋ1 cell lines during matrix detachment at 6 days. e. Impact of GSK J4 (7.5µM) on expression of various surface markers of stemness in HeLa, HCT116 and 22Rʋ1 cell lines during matrix detachment at 6 days. f. Enrichment of KDM6B and RNA Pol II on the promoters of SOX2 and CD44 genes both in the presence and absence of GSK J4 (7.5µM) at 6 days, non-immune IgG was used input control. g . Western blot showing GSK J4 (7.5µM) treatment for 6 days significantly induces the expression of H3K27me2/3 in 22Rʋ1 during matrix detachment condition. h. As per the above-mentioned conditions global H3K27me2/3 levels in GSK J4 (7.5µM) in 22Rʋ1 during matrix detachment condition.
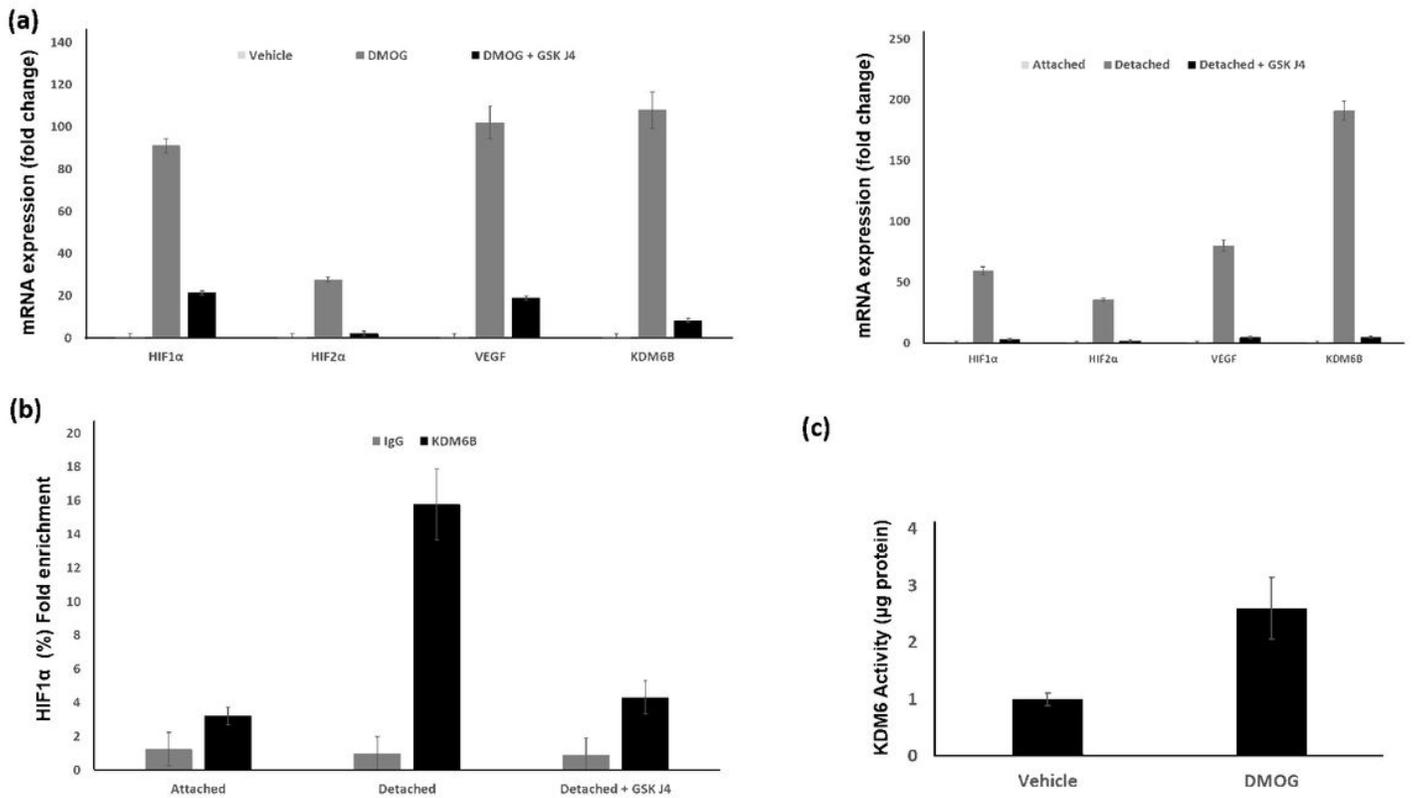
Figure 3

KDM6B regulates the expression of HIF 1α in cancer cells during matrix detachment. a. mRNA expression of various HIF 1α, HIF2 α, VEGF and KDM6B in presence of DMOG and matrix detachment alone or in combination of GSK J4 (7.5µM) in HeLa cells during matrix detachment at 6 days. The values were normalized with housekeeping gene RPLP0 and further gene expression values were calculated. b. Enrichment of KDM6B on the promoters of HIF 1α both in the presence and absence of GSK J4 (7.5µM) in HeLa cells during matrix detachment at 6 days, non-immune IgG was used input control. c. Impact of GSK J4 (7.5µM) a specific inhibitor of KDM6 histone demethylases on KDM6 activity in nuclear extracts of HeLa cells during matrix detachment at 6 days.
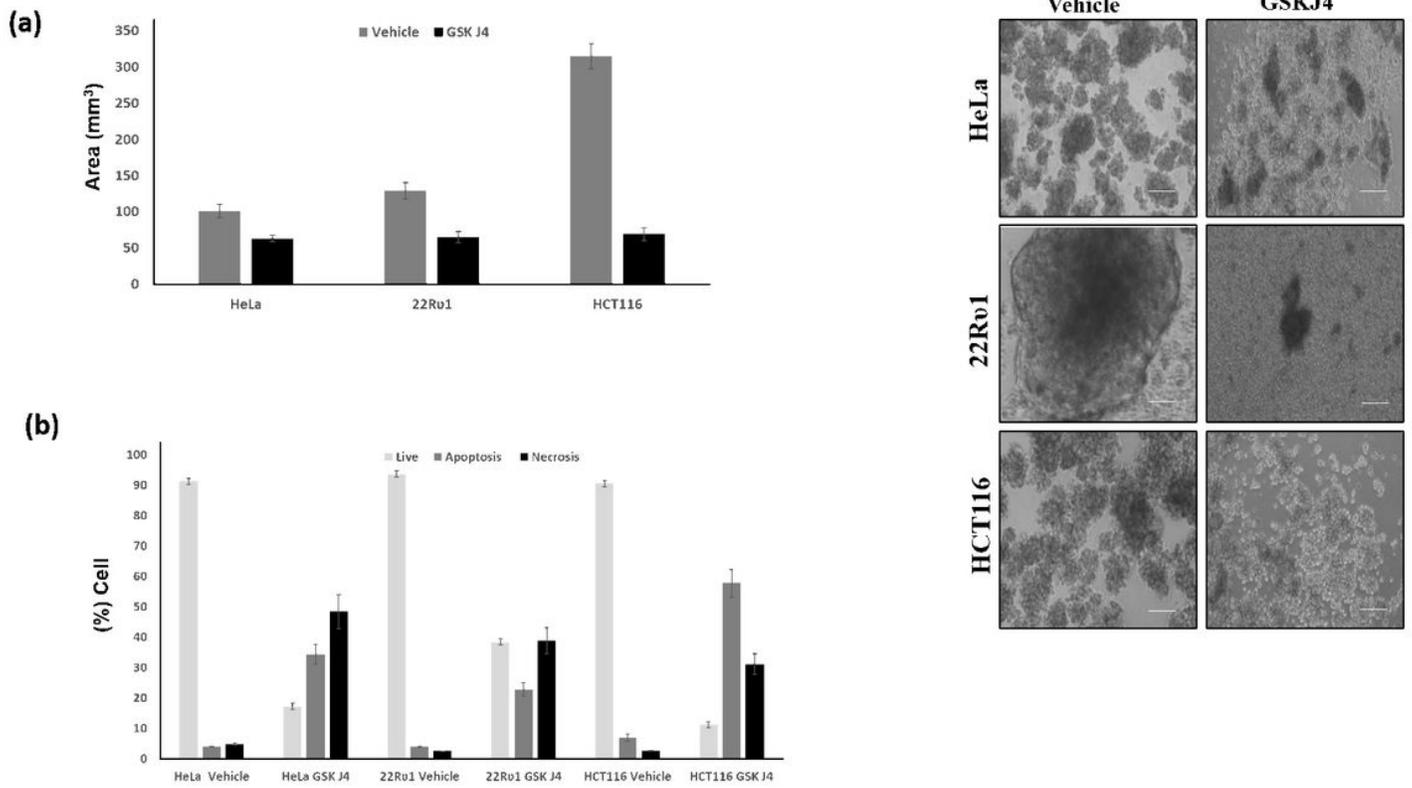
Figure 4

Clinical correlation of KDM6B and HIF 1α in various cancer. Correlation analysis of gene expression between KDM6B and HIF 1α from metastatic samples. (A) Gene expression in metastatic melanoma samples. (B) Gene expression in metastatic breast samples.
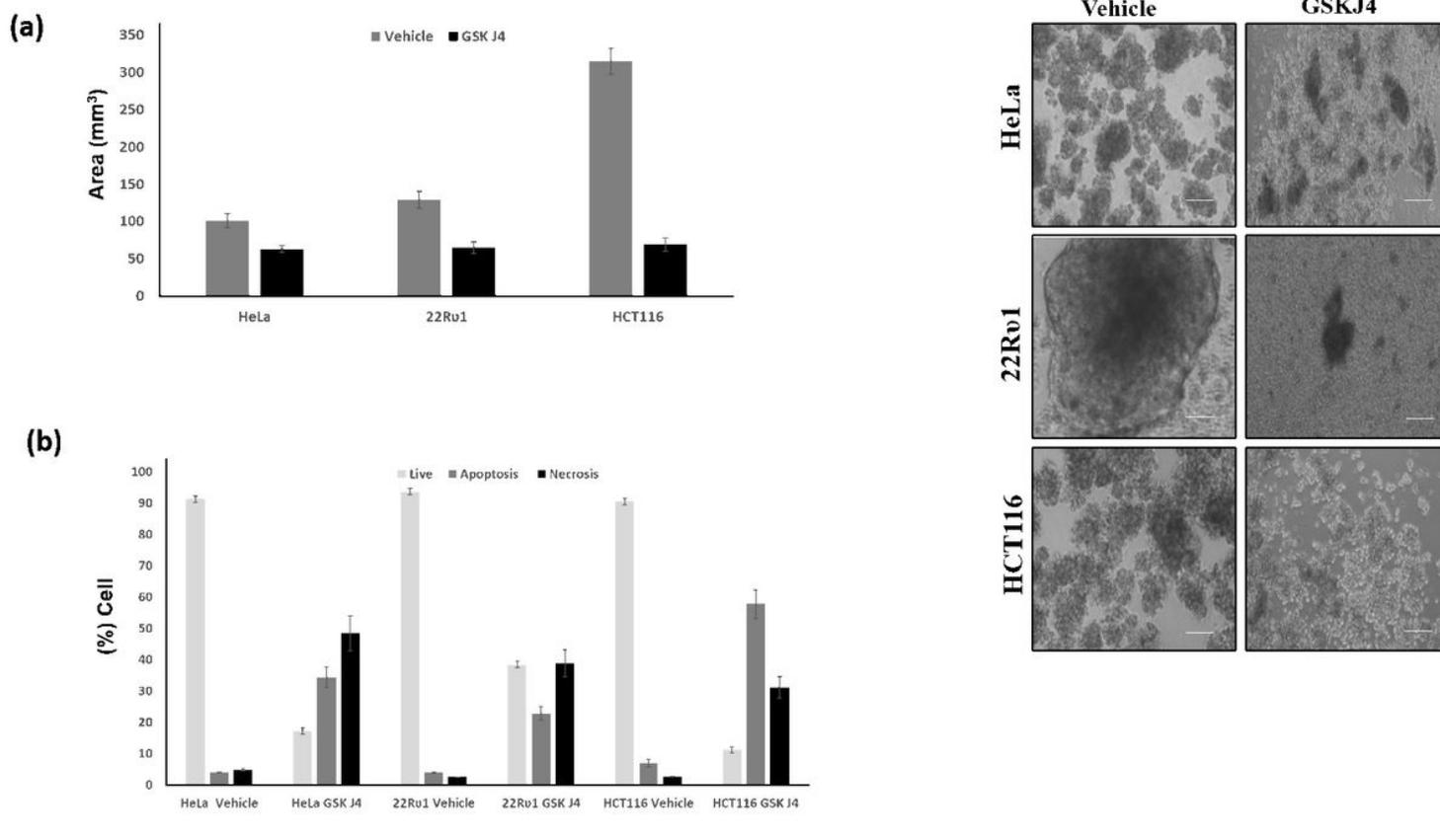
Figure 5

Targeting KDM6B reduces spheres formation capacity and promotes cell death in matrix detached cancer cells. a. Sphere formation assay HeLa, HCT116 and 22R⬜1 cell lines were cultured in matrix detachment for 6 days and simultaneously treated either with GSK J4 (7.5µM) or with vehicle (control). At the end of treatment schedule sphere images were captured by using Nickon inverted light microscope and images were analyzed for size measurement by image J software N=8. Histogram plots were plotted for average size in all conditions. b. As above mentioned, similar treatment strategy was used and apoptosis assay was done by using Annexin V and PI. The histogram data was plotted for % cells showing live or apoptotic populations.

Supplementary Files

This is a list of supplementary files associated with this preprint. Click to download.

- SupplementaryFigures.pdf